RSC Advances

ROYAL SOCIETY OF CHEMISTRY

www.rsc.org/advances

Understanding in Crystallization of Polyethylene: The Role of boron nitride (BN) particles

Xianlong Zhang[1, 2], Hong Wu[1*], Shaoyun Guo[1*], Yuzhong Wang[2]

1 The State Key Laboratory of Polymer Materials Engineering, Polymer Research Institute of Sichuan University, Chengdu 610065, China

2 Center for Degradable and Flame-retardant Polymeric Material, Sichuan University, Chengdu 610064, China

ABSTRACT: In an attempt to correctly understand an extra weak exothermic peak (T_h) (near the melting temperature of the polyethylene (PE)) of the PE in the PE/boron nitride (BN) composites, a new hypothesis was proposed and proved: T_h was induced by PE crystallization. When the BN content was more than 10 wt%, the T_h was observed. Simultaneously, beside the T_h, another weak exothermic peak (T^1_h), was also found. Beside the main melting peak (T_m), an extra melting peak (T_{mh}) also appeared. The results of the local thermal analysis technique (nano-TA) showed that the local melting temperature (nano-T_m) of the PE near the BN aggregates was higher 4-8 °C than that in other areas, indicating that the meso-phase (meso-phase was also induced by PE crystallization) can be formed near the BN aggregates during the PE crystallization. Moreover, the appearance of the T_h and T^1_h was attributed to the differently nucleated capability of the different BN aggregates in local areas during the PE crystallization. When the annealing time and temperature were 20 min and 130

* To whom correspondence should be addresses. (Prof. Wu, Email: wh@scu.edu.cn, Fax: 86-028-85466077)
* To whom correspondence should be addresses. (Prof. Guo, Email: sguo@scu.edu.cn, Fax: 86-28-85405135)

°C, respectively, the thermal conductivity of the PE/BN composite was 16% higher than that of the unannealed PE/BN composites. In addition, the results of the Wide angle X-ray diffraction (WAXD) showed that the BN particles had no influence on the PE crystal form in the PE/BN composites.

Key words: Nano-TA analysis, Crystallization, Polyethylene, Boron nitride

1. INTRODUCTION

Polyethylene (PE) was one of the most important thermoplastic polymers owing to its low manufacturing cost and rather versatile properties. It was used for applications ranging from packaging to furniture, as well as to agricultural films.[1-5] In order to enhance mechanical, thermally conductive and electrical properties of the PE, a wide variety of inorganic fillers such as metallic particles, [6] ceramic fillers, [7] graphite, [8-9] and carbon nanotubes was utilized. [10] Among these fillers, graphite was usually recognized as the best thermally conductive filler because of its good thermal conductivity and low cost.

Recently, increasing attention had been paid to the use of exfoliated graphite [11-13] and exfoliated graphite nano-platelets (GNPs) [14-19] in polymers to fabricate thermally conductive nano-composites, since the thermal conductivity of single graphene sheets constituting graphite was theoretically estimated to be as high as 5300 W/mK. [20] Wu et al. prepared low-density polyethylene (LDPE)/low-temperature expandable graphite (LTEG) composites by an in situ expansion melt blending process. [21] The experimental result showed that thermal conductivity of the LDPE/LTEG composites

with 60 wt% LTEG was increased by 23 times in comparison with that of the pure LDPE, and it increased from 0.47 to 11.28 W/mK. Meanwhile, it was interesting to note that when the graphite content was more than 20 wt%, an extra and unexpected weak exothermic peak (T_h), which was very close to T_m and 8-12 ^{o}C higher than T_c, appeared. Since both the highest T_c and appearance of the T_h occurred at 20 wt% LTEG, they presumed that the percolation threshold concentration may lie around this value, indicating the T_h may be related to the fillers network structure in the composites.

Similar phenomenon had been also found by Zheng et al., and this extra exothermic peak (T_h) for the high-density polyethylene (HDPE) filled with graphite (GP) could be attributed to the increased particle agglomeration during the cooling and the surface inactivity of GP. The polymer-filler interface decreased, since the shrink of HDPE accompanied the GP particles agglomeration during the cooling. They proposed that such decrease of the polymer-filler interface should accompany the weak exothermic behavior, resulting in the appearance of the extra exothermic peak at T_h. Therefore, they suggested that the main reason for the appearance of the T_h was the particle aggregation and the change of the temperature, which accompanied the decrease of interface between particles and HDPE matrix. [22] However, this result had not been confirmed through rigorous and logical the experimental data. Therefore, it was only a hypothesis, and this extra exothermic peak was necessary to be further investigated.

Beside the graphite, in recent years, hexagonal boron nitride (BN), which was

similar to the graphite structure, also attracted much more attention because of its excellent mechanical strength, highly electrical insulating, and highly thermally conducting nature.[23-26] However, when the high concentration BN particles were added into PE matrix, whether such extra exothermic peak (T_h) could also appear? How the BN particles affected the crystallization and melting behavior of the PE? The traditional characterization methods, for example, Differential Scanning Calorimetry (DSC), only can give a whole understanding about the crystallization and melting of the polymer. Generally, the dispersion state of the fillers had strong effect on crystallization and melting of the polymer in the local areas. Therefore, it was necessary to understand the effect of the fillers on crystallization and melting of the polymer in the local areas. However, it was difficult to study the effect of the BN on the crystallization and melting of the PE in the local areas because of the limitation of the characterization methods.

Fortunately, a local thermal analysis technique (nano-TA) utilizing scanning force microscopy was developed. [27] This technique was an analogy of mesoscopic thermo-mechanical analysis of which penetration depth of loaded needle was measured as a function of temperature. This technique was performed by a specially designed probe to contact with the sample surface, heating the end of the cantilever, and measuring its deflection using the standard beam detection of AFM. At the glass transition temperature (T_g) or melting temperature (nano-T_m), the polymer sample surface was soften, which not only allowed the cantilever with small normal load to indent the surface of the sample, but also enabled the probe to penetrate the sample

and decrease the deflection of the cantilever. The change in slope of the deflection signal was an indication of a thermal transition. [28] Therefore, the nano-TA was useful to characterize the effect of the BN particles on the melting behavior of the PE in local areas.

In this study, in an attempt to correctly understand an extra and unexpected weak exothermic peak (T_h) of the PE, which was very close to T_m and 8-12 °C higher than T_c. The BN particles were added into PE matrix through melt compounding. The melting and crystallization behavior of the PE/BN was investigated through Differential Scanning Calorimetry (DSC) and (Wide angle X-ray diffraction) WAXD, the local melting behavior of the PE/BN composites in nano-scale was studied by the nano-TA. Moreover, based on above investigations, the crystallization behavior of the PE matrix was controlled through investigating the optimal annealing temperature so as to enhance the thermal conductivity of the PE/BN composites.

2. EXPERIMENTAL SECTION

2.1 Materials and preparation of the PE/BN composites

A commercial high density polyethylene (PE) (5000s) with melt index (MI) = 1 g/10 min (2.16 kg, 190 °C) was supplied by Qilu Petrochemical Co., Ltd. (China). The boron nitride (BN) with a particle size of 3~5 μm was purchased from Shandong Pengcheng Special Ceramics Co., Ltd. (China). PE and BN particles were compounded in an internal mixer (Haake Rheocord 90, Gebr. Haake GmbH, Karlsruhe, Germany) at 180 °C for 8 min, and the rotate speed was 30 rpm.

2.2 DSC Analysis

Melting and crystallization behaviors of the PE/BN composites were measured by a TA-Q20 (USA) thermal system purged with nitrogen. The program for DSC measurement was run from 25 to 180 ˚C, which was the first heating scan. After the sample was equilibrated at 180 ˚C for 3 min to erase previous thermal and stress history, it was cooled to 25 ˚C, and then heated again to 180 ˚C for the second heating scan.

2.3 Wide angle X-ray diffraction (WAXD)

The crystalline structure of the PE/BN composites were investigated using a wide angle X-ray diffraction (WAXD, Panalytical X' pert PRO diffractometer with Ni-filtered Cu Kα radiation, The Netherlands). The continuous scanning angle range used in this study was from 10° to 35° at 40 kV and 40 mA.

2.4 Nano-TA

The sample for nano-TA test was cut by a microtome (Leica Microsystems purged with liquid nitrogen) with vertical cross section. The sample was cut into a size of 0.8 mm× 4 mm, and the thickness of the sample was 10 μm.

A nano-TA add-on (Anasys Instruments) combined with E-sweep Lorentz Contact Resonance Imaging for Atomic Force Microscopes (LCR-AFM) instruments (SII Co. Ltd.) was used to characterize the morphology of the PE/BN composites. An AN-2 silicon thermal probe was used (spring constant: 1.0 N/m, resonance frequency: 59 kHz). Local thermal analysis measurements were obtained using a temperature ramp of 1200 ˚C/min from 25 ˚C up to the penetration temperature under vacuum

(below 5.0×10^{-4} Pa). AFM topographic and amplitude images with area of 400 and100 μm^2 were obtained. Temperature was calibrated through two semi-crystalline polymers with known melting temperature at 60 ˚C (polycaprolactone) and 238 ˚C (polyethylene terephthalate).

2.5 Thermal conductivity measurement

A thermal constants analyzer (Hot Disk thermal conductivity detector, 1500) produced by Hot Disk Company (Sweden) was utilized to measure the thermal conductivity of the PE/BN composites. The thermal constants analyzer used the transient plane source (TPS) method to measure the thermal conductivity of materials. The TPS method used the Fourier Law of heat conduction as its fundamental principle, and the uncertainties were about 5%.

3. RESULTS AND DISCUSSION

3.1 DSC analysis

Figure 1 showed the effect of the BN content on the crystallization behaviors of the PE/BN composites, and the cooling rates were 10 (as shown Figure 1(a)) and 2 ^{o} C/min (Figure 1 (b)), respectively. According to Figure 1 (a), compared to the neat PE, the crystallization temperature (T_c) of the PE in the PE/BN composites remarkably shifted to the high temperature. Simultaneously, the more BN content was, the higher crystallization starting temperature (T_{onset}) and T_c of the PE in the PE/BN composites were. Apparently, BN, which liked a lot of fillers, was a nucleating agent of the PE crystallization. Therefore, the incensement of the T_c and T_{onset} can be attributed to the heterogeneous nucleation effect of BN particles for PE crystallization. Meanwhile, it

was interesting to note that when the BN content was more than 10 wt%, an extra and unexpected weak exothermic peak (T_h) appeared as shown in Figure 1 (a). The similar phenomenon was also found by Wu et al. in low-density polyethylene/low-temperature expandable graphite composites, and they the T_h may be related to the fillers network structure in the composites. [21]

Moreover, the similar observation had been also reported by Zheng et al. for HDPE/graphite composites, they attributed the appearance of T_h to the increased particle agglomeration during the cooling and the surface inactivity of the graphite. [22] Wu and Dong et al agreed that the T_h was not induced by PE crystallization because the T_h was very closed to T_m, and 8-12 ^{o}C higher than T_c. If the mentioned above theories that proposed by Wu and Dong et al was right, the cooling rates had little effect on T_h. However, compared to the 10 ^{o}C/min, when the cooling rate reduced to 2 ^{o}C/min, the T_h became more obvious. Meanwhile, when Figure 1(b) was enlarged in local area as shown in Figure 2, beside the T_h, another unexpected weak exothermic peak, which was defined as T^1_h, was found. Moreover, the T_h for the PE/BN composites was also observed in Figure 2 when the BN content was 10 wt%. According to the theories that proposed by Wu and Dong et al, it was difficult to understand the results of the Figure 1 (b) and Figure 2. Therefore, the new understanding of the T_h was necessary. According to effect of the cooling rates on the T_h, a new hypothesis was proposed: T_h was induced by PE crystallization.

In order to correctly understand the T_h and T^1_h, the melting behavior of the PE/BN composites was investigated. Figure 3 showed the effect of the content of BN

on the melting behaviors of the PE/BN composites, and the heating rates were 10 and 2 °C/min，respectively. From Figure 3 (a), it can be seen that the BN concentration had significant influence on the melting temperature of the PE, and the peak melting temperature (T_m) gradually shifted toward a lower temperature with increasing BN loading. For example, T_m for the neat PE was observed at 130.2 °C (the heating rate was 2 °C/min), whereas it decreased by about 3.5 °C for the composite with 50 wt% BN. According to literature report [29, 30], the incorporation of BN particles can hinder the mobility of PE macromolecular chains during the crystallization process, resulting in formation of imperfect crystallites with small size and thin lamellar. Therefore, the T_m of the PE reduced when the high concentration of BN particles was loaded into PE matrix. Meanwhile, beside the main melting peak (T_m), it was interesting to note that when the BN content reached to 50 wt%, an extra and unexpected weak melting peak (T_{mh}) appeared as shown in Figure 3 (a). When the heating rate was 2 °C/min, the more obvious T_{mh} for the PE/BN composites (30 wt% and 50 wt% BN content) was observed, indicating that the meso-phase (meso-phase was also induced by PE crystallization) can be formed in the PE/BN composites (30 wt% and 50 wt% BN content).

The crystallinity of the PE in the PE/BN composites was calculated by its melt enthalpy with follow equation:

$$X_c = \Delta X_c / (W_{PE} * \Delta X_c^0)$$

Where X_c was crystallinity of the PE in the PE/BN composites, ΔX_c was melting enthalpy of the PE in the PE/BN composites, ΔX_c^0 was melting enthalpy of

completely crystalline PE (245.3 J/g),[21] W_{PE} was the mass fraction of the PE in the PE/BN composite.

Table 1 showed the crystallinity (X_c) and melting point (T_m) of the PE in the PE/BN composites under different heating rates (2 and 10 ^oC/min). As listed in Table 1, compared to the neat PE, the X_c of PE roughly decreases with increasing BN content, which was the result of a compromise between the nucleating and the retarding effects of the BN particles on the polymer matrix during non-isothermal crystallization.[14] The inhibited effect of BN particles on diffusion of PE macromolecular chains to the growing crystallites may be more predominate than their heterogeneous nucleation effect on facilitating the crystallization so that the X_c reduced with increasing the BN content.

If the new hypothesis, which the T_h was induced by PE crystallization, was right, the annealing time at T_h had significant effect on melting behavior of the PE in the PE/BN composites. Figure 4 showed the effect of annealing time on the melting behaviors of the PE/BN composites, and the annealing temperature, which was close to T_h, was 131 ^oC. The neat PE was also annealed with the same conditions, and all the heating rates were 2 ^oC/min. According to Figure 4 (a), the T_{mh} of the PE/BN composites remarkably shifted to a high temperature with increasing the annealing time, indicating that the meso-phase (meso-phase was also induced by PE crystallization) of the PE can be formed in the PE/BN composites at T_h with increasing the annealing time. Simultaneously, the longer annealing time was, the more obvious T_{mh} was. Therefore, after the annealing of the PE/BN composite at T_h,

the melting behavior of the PE in the PE/BN composite had obviously changed, which proved the new hypothesis (the T_h was induced by PE crystallization) was right. Meanwhile, no matter how long the annealing times, the neat PE melting behavior almost had no change. Therefore, the addition of the BN particles significantly changed the PE crystallization and melting behavior so that it was necessary to further investigate the role of the BN particles during the PE crystallization and melting.

Wide angle X-ray diffraction (WAXD) analysis

According to above studies, the new crystallization peak (T_h) and the new melting peak (T_{mh}) were observed during the PE in the PE/BN composite crystallization and melting process. The T_h and T_{mh} may correspond to the change of the crystalline structure of the PE. Therefore, it was necessary to reveal the effect of the BN particles on the crystalline structure of the PE. The crystalline structure of the PE/BN composites was characterized by WAXD and the results were shown in Figure 5. As shown in Figure 5, the neat PE had two intense diffraction peaks at $2\theta = 21.6^o$ and 23.8^o, which corresponded to the (110) and (221) crystal planes, respectively. For the BN particles, the peak at $2\theta = 26.8^o$ corresponding to the (002) crystal plane. Beside the stack peaks of the PE and BN particles, no new peak was found when the BN particles were loaded into PE matrix, indicating that the new crystal was not formed. Therefore, the BN particles had no influence on the PE crystalline form in the PE/BN composites.

Nano-TA analysis

Figure 6 showed the Lorentz Contact Resonance Imaging for Atomic Force

Microscopes (LCR-AFM) images of the PE/BN composites. The morphology of the PE/BN composites (30 wt % BN content) was obtained through LCR-AFM as shown in Figure 5(a) (height image) and 5(b) (amplitude image). It was clearly observed that most of the BN particles existed in the form of aggregates, and few independent BN particles existed. During the traditional DSC testing for the PE/BN composites, the crystallization and melting of polymer occurred simultaneously with increasing temperature, since the crystallization of the polymer was imperfect. In order to eliminate the effect of crystallization and melting of the PE, which occurred simultaneously, the heating rates was as high as 1200 °C /min during the nano-TA testing. The local thermal analysis data of the assigned positions were measured by nano-TA, and the nano-T_m=126.8±7.9 °C as shown in Figure 7. According to Figure 6(c), it was noted that the T_m of the PE in local area reached to 145.1 °C, indicating that the crystallization of the PE at T_h (135.1 °C) was possible as shown in Figure 4(a). To confirm the reliability of the nano-TA testing, the T_m of the PE in the PE/BN composites (30 wt%) was measured by the traditional DSC analysis, and the T_m was 131.3 °C. Although the nano-T_m was not the same as the T_m, it was close. Therefore, the local thermal analysis data of the nano-TA for the PE/BN composites was reliable and reasonable.

In order to further confirm the T_m of the PE in the PE/BN composites, the special areas were chosen for nano-TA testing as shown in Figure 8(a) and 8(b). The aggregates of the BN particles were in the areas of the A, D and E. Meanwhile, the areas of the B and C almost had no the BN particles. The values of the nano-T_m were

shown in the Figure 8(d). It was found that the nano-T_m in the areas of the A, D and E were 4-8 °C higher than that in the areas of the B and C, indicating that the nano-T_m of the PE near the BN aggregates was higher than that in other areas. Combined with the results of the Figure 4, the meso-phase of the PE can be formed near the BN aggregates at the T_h during the PE crystallization. According to Figure 8(a) and 8(b), the nano-T_m in the areas of the A, D and E were different because the dispersion states of the BN particles were different. Similarly, the appearance of the T_h and T^1_h was resulted from the differently nucleated capability of the different BN aggregates in local area. In addition, the changes in slope of the deflection signal for two lines (black lines), which corresponded to k1 and k2 points in Figure 8(a), respectively, were not observed as shown in the Figure 8(c), indicating that the thermal transition did not exist at these two points. That was because in the areas of the A and D, these two testing points exactly existed at the BN particles. Conversely, it was also proved that the other data points of the assigned positions for nano-TA testing can reliably exhibit the nano-T_m of the PE in the PE/BN composites.

According to the results of the Figure 4(a), the T_{mh} reached to 137 °C. To prove the thick lamellar of the PE near the BN aggregates, the effect the measurement distance on the T_m of the PE was investigated as shown in Figure 9. The point (**a)** had the highest nano-T_m than other points, and reached to 135.2 °C. Compared to the nano-T_m of the points (**a**), the nano-T_m remarkably shifted to low temperature with increasing the measurement distance. The nano-T_m of the PE changed slightly in comparison with that of the points (**a**) and (**b**) as shown in Figure 8(c) and Figure 8(d)

when the measurement distance reached to 1.4 μm (point (**c**)),. This result proved that the meso-phase of the PE was near the BN aggregates.

Thermal conductivity of the PE/BN composites

Base on above investigations, the crystallization behavior of the PE matrix was controlled through investigating the optimal annealing temperature so that the thermal conductivity of the PE/BN composites can be enhanced.

Figure 10(a) showed the thermal conductivity of the PE/BN composites and pure PE at different annealing time and temperature. When the annealing temperatures were 140 ^{o}C, 130 ^{o}C and 120 ^{o}C, the thermal conductivity of the pure PE changed slightly. However, the thermal conductivity of the PE/BN composites remarkably enhanced with the annealing time increasing when the annealing temperatures were 130 ^{o}C and 120 ^{o}C. Particularly, when the annealing time and temperature were 20 min and 130 ^{o}C, the thermal conductivity of the PE/BN composites was 16 % higher than that of the unannealed PE/BN composites. Meanwhile, when the annealing temperature was 140 ^{o}C, the thermal conductivity of the PE/BN composites and the PE crystallinity in the PE/BN composites changed slightly with the annealing time increasing as shown in Figure 10(b). This result was ascribed that the PE matrix was in melting state during annealing. Moreover, when the annealing temperatures were 130 and 120 ^{o}C, the PE crystallinity in the PE/BN composites increased with the annealing time increasing so that the thermal conductivity of the PE/BN composites were enhanced. Interestingly, the 130 ^{o}C annealing temperature was more effective to enhance the thermal conductivity of the PE/BN composites than other temperatures as

shown in Figure 7(a). In addition, the results of the Figure 1 indicated that the meso-phase (high melting temperature) of the PE in the PE/BN composites can be formed during annealing at 130 ^{o}C. To combine the results of the Figure 7, it was found that the meso-phase was more helpful to enhance the thermal conductivity of the PE/BN composites.

4. CONCLUSIONS

In this paper, the crystallization and melting behavior PE/BN composites was investigated. When the BN content was more than 10 wt%, an extra and unexpected weak exothermic peak (T_h) was observed. The T_m and X_c of the PE in the PE/BN composites reduced when the high concentration of BN particles was loaded into PE matrix. Beside the main melting peak (T_m), it was interesting to note that when the BN content reached to 50 wt%, an extra and unexpected weak melting peak (T_{mh}) appeared. In addition, the cooling rates had significantly effect on the T_h, and the annealing time at T_h had also remarkable influence on the T_{mh}. The nano-T_m of the PE near the BN aggregates was higher 4-8 ^{o}C than that in other areas, indicating that the meso-phase of the PE can be formed near the BN aggregates during the PE crystallization. The appearance of the T_h and T^1_h resulted from the different nucleated capability of the different BN aggregates in local area. When the annealing time and temperature were 20 min and 130 ^{o}C, the thermal conductivity of the PE/BN composites was 16 % higher than that of the unannealed PE/BN composites. In addition, the results of the WAXD showed that the BN particles had no influence on

the PE crystal form in the PE/BN composites.

ACKNOWLEDGMENTS

Financial supports of the National Natural Science Foundation of China (51273132, 51227802 and 51121001), the Program for New Century Excellent Talents in University (NCET-13-0392), the Sichuan Province Youth Science Fund (2015JQ0015) and the China Postdoctoral Science Foundation (2015M572474) are gratefully acknowledged.

REFERENCES

1. Meille, S. V.; Bruckner, S.; Porzio, W. *Macromolecules*, **1990**, *23*(18), 4114-4121.
2. Lotz, B.; Graff, S.; Straupe, C.; Wittmann, J. C. *Polymer*, **1991**, *32*(16), 2902-2910.
3. Haggenmueller, R.; Fischer, J. E.; Winey, K. I. *Macromolecules,* **2006**, *39*(8), 2964-2971.
4. Haggenmueller, R.; Guthy, C.; Lukes, J. R.; Fischer, J. E.; Winey, K. I. *Macromolecules*, **2007**, 40(7), 2417-2421.
5. Di Lorenzo, M. L.; Avella, M.; Avolio, R.; Bonadies, I.; Carfagna, C.; Cocca, M.; Maria E. E.; Gentile, G. *J. Appl. Polym. Sci*. **2012**, *125*(5), 3880-3887.
6. Kumlutas, D.; Tavmana, I.H.; Coban, M.T. *Compos. Sci. Technol.,* **2003**, *63*(1), 113–117.
7. Yu, S.; Hing, P.; Hu, X. *Compos. Part: A,* **2002**, *33*(2), 289–292.
8. Ye, C.M.; Shentu, B.Q.; Weng, Z.X. *J. Appl. Polym. Sci.,* **2006**, *101*(6), 3806–3810.
9. Tu, H.; Ye, L. Polym. *Adv. Technol.*, **2009**, 20(1), 21–27.
10. Patton, R. D.; Pittman, C. U.; Wang, L.; Hill, J. R.; Day, A. *Compos. Part A*, **2002**, *33*(2), 243–245
11. Moisala, A.; Li, Q.; Kinloch, I. A.; indle, A. H. *Compos. Sci. Technol.* **2006**, 66(10),

1285-1288.

12. Mu, Q.; Feng, S. *Thermochim. Acta.* **2007**, 462(1–2), 70-75.

13. Debelak, B.; Lafdi, K. *Carbon*, **2007**, *45*(9), 1727-1734.

14. Ghose, S.; Watson, K. A.; Working, D. C.; Connell, J. W.; Smith, J. G.; Sun, Y. P. *Compos. Sci. Technol.* **2008**, *68*(7 – 8), 1843-1853.

15. Tang, Z.; Kang, H.; Shen, Z.; Guo, B.; Zhang, L.; Jia, D. *Macromolecules*, **2012** *45*(8), 3444-3451.

16. Kalaitzidou, K.; Fukushima, H.; Drzal, L. T. *Carbon*, **2007** *45*(7), 1446-1452.

17. Jiang, X.; Drzal, L. T. *Polym. Compos*, **2012**, *31*(6), 1091-1098.

18. Yu, A.; Ramesh, P.; Itkis, M. E.; Bekyarova, E.; Haddon, R. C. *J. Phys. Chem. C* **2007**, 11(21):7565-7569.

19. Veca, L. M.; Meziani, M. J.; Wang, W.; Wang, X.; Lu, F.; Zhang, P.; Sun, Y. P. *Adv. Mater* **2009**, 21(20), 2088-2092.

20. Balandin, A. A.; Ghosh, S.; Bao, W.; Calizo, I.; Teweldebrhan, D.; Miao, F.; Lau, C. N. *Nano. Lett.* **2008**, 8(3), 902 – 907.

21. Wu, H.; Lu, C.; Zhang, W.; Zhang, X. *Mater. Des.* **2013**, 52, 621-629.

22. Dong, Q.; Zheng, Q.; Zhang, M. *J. Mater. Sci,* **2006**, *41*(10), 3175-3178.

23. Zhi, C.; Bando, Y.; Terao, T.; Tang, C.; Kuwahara, H.; Golberg, D. *Adv. Funct. Mater.* **2009**, *19*(12), 1857-1862.

24. Li, Y.; Luo, Z.; Tung, S.; Schneider, E.; Wu, J.; Li, X. *Nanoscale. Res. Lett.* **2011**, *6*(1), 1-7.

25. Martin-Gallego, M.; Verdejo, R.; Khayet, M.; de Zarate, J. M. O.; Essalhi, M.; Lopez-Manchado, M. A. *Nanoscale. Res. Lett.* **2011**, *6*(1), 1-7.

26. Zhang, X.; Shen, L.; Wu, H.; Guo, S. *Compos. Sci. Technol.* **2013**, *89*, 24-28.

27. Mueller, T. *Mater. Today* **2009**, 12, 40−43.

28. Tanji, N.; Wu, H.; Kobayashi, M.; Takahara, A. *Macromolecules,* **2013**, *46*(24), 9722-9728.

29. Krupa, I.; Novák, I.; Chodák, I.. *Synth. Mater*, **2004**, *145*(2), 245-252.

30. Zhou, W.; Wang, C.; Ai, T.; Wu, K.; Zhao, F.; Gu, H. *Compos. Part A:* **2009**, 40(6), 830-836.

Table 1 The crystallinity (X_c) and melting point (T_m) of the PE in the PE/BN composites under different heating rates (2 and 10 °C/min).

Samples	2 ℃/min		10 ℃/min	
	X_c	T_m	X_c	T_m
Neat PE	60.6	133.7	59.6	133.8
10 wt% BN	59.7	133.2	58.2	133.3
30 wt% BN	58.6	132.4	59.4	132.6
50 wt% BN	47.6	130.2	45.7	130.8

Figure caption

Figure 1 the effect of the BN content on the crystallization behaviors of the PE/BN composites. The cooling rates were 2 and 10 °C/min, respectively.

Figure 2 the enlarged figure according to Figure 1(b). The cooling rate was 2 °C/min, and the scale was from 125 to 145 °C.

Figure 3 the effect of the BN content on the melting behaviors of the PE/BN composites. Heating rates were 2 and 10 ^{o}C /min，respectively.

Figure 4 the effect of annealing time on the melting behaviors of the PE/BN composites, and the neat PE was also annealed at 130 ^{o}C. All the heating rates were 2 ^{o}C/min.

Figure 5 the PE/BN composites of the Wide angle X-ray diffraction (WAXD) profiles.

Figure 6 the Lorentz Contact Resonance Imaging for Atomic Force Microscopes (LCR-AFM) images of the PE/BN composites: (a) LCR-AFM height image; (b) LCR-AFM amplitude image; (c) Local thermal analysis data of the assigned positions were obtained by nanoTA, and all the heating rates was 1200 ^{o}C/min; (d) The DSC data of the PE/BN composites, and the heating rate was 2 ^{o}C/min.

Figure 7 the map of the nano-T_m distributions obtained from Figure 6(c).

Figure 8 LCR-AFM images of the PE/BN composites: (a) LCR-AFM height image; (b) LCR-AFM amplitude image; (c) Local thermal analysis data of the assigned positions were obtained by nanoTA; (d) the nano-Tm of the PE in the local areas.

Figure 9 LCR-AFM images of the PE/BN composites: (a) LCR-AFM amplitude image; (b) LCR-AFM height image; (c) Local thermal analysis data of the assigned positions were obtained by nano TA; (d) effect of the measurement distance on the thermal transition temperature of the composites.

Figure 10(a) the thermal conductivity of the PE/BN composites and pure PE at different annealing time and temperature; (b) the crystallinity of the PE in the PE/BN composites and neat PE at different annealing time and temperature.

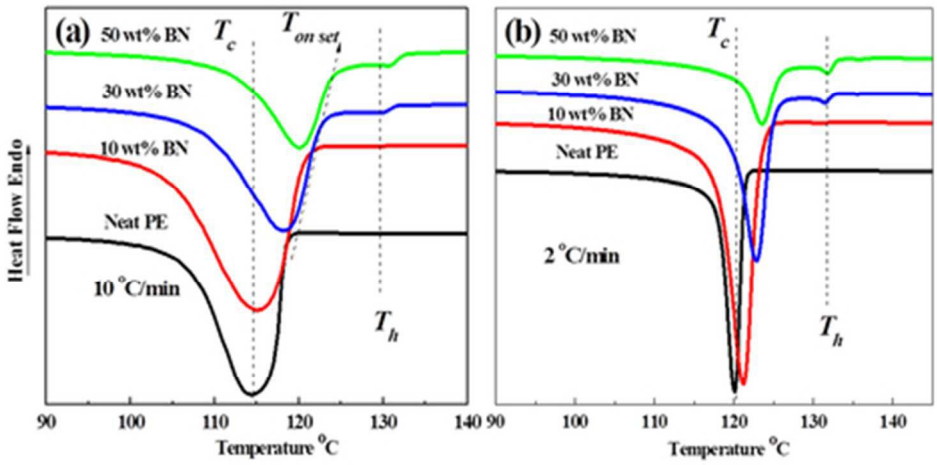

39x19mm (300 x 300 DPI)

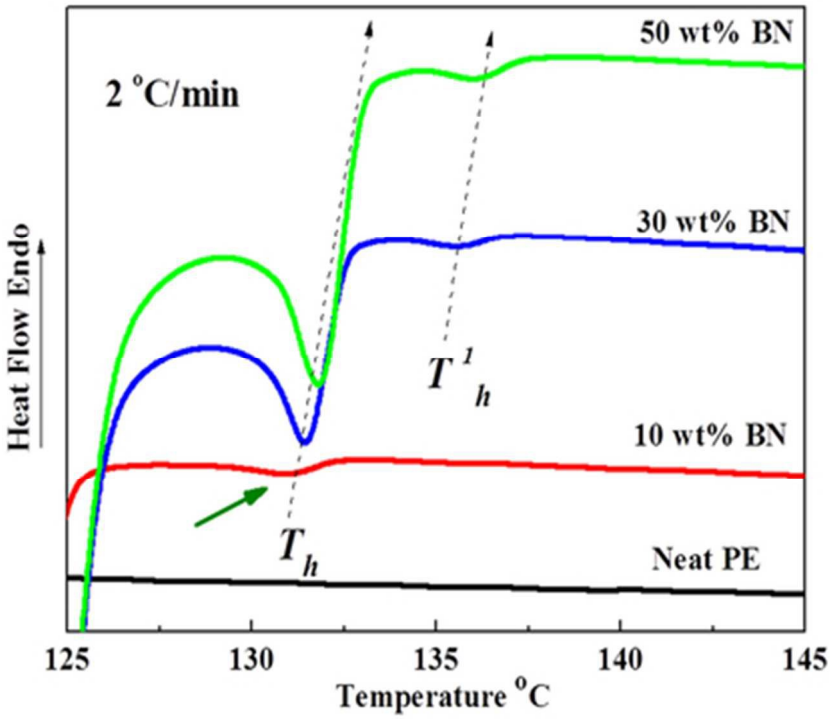

34x30mm (300 x 300 DPI)

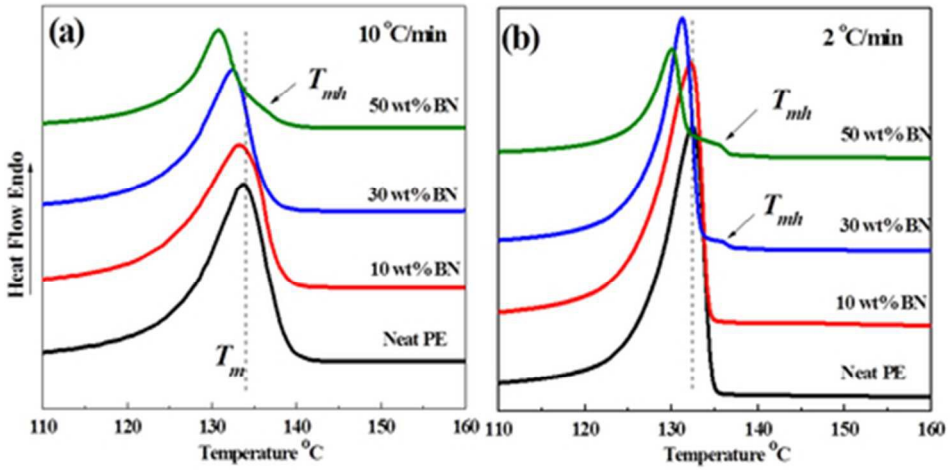

39x19mm (300 x 300 DPI)

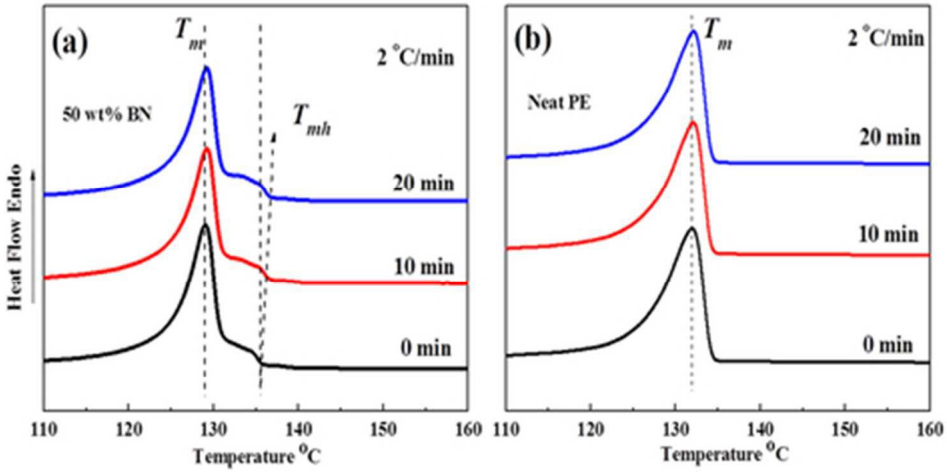

39x19mm (300 x 300 DPI)

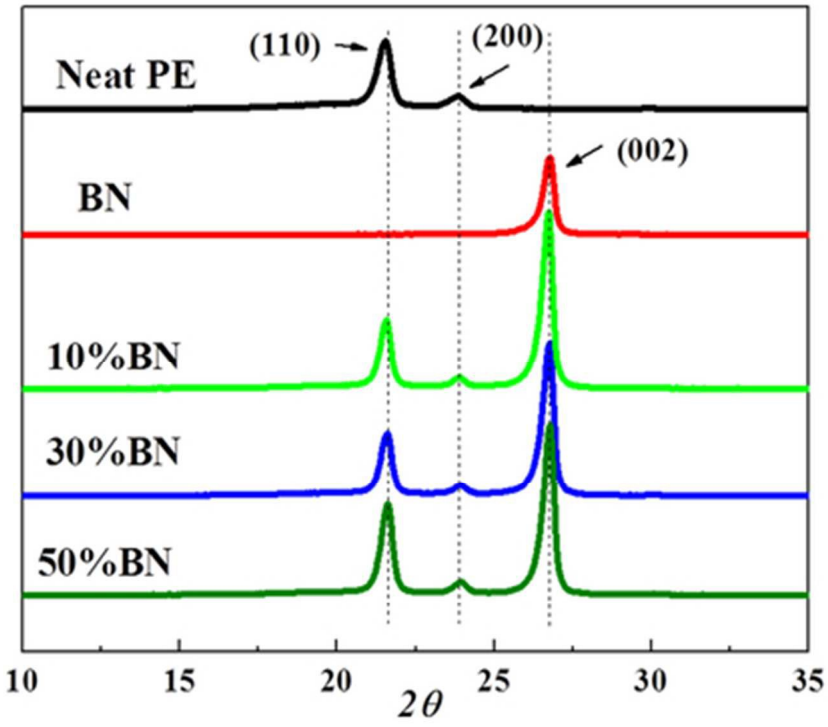

34x30mm (300 x 300 DPI)

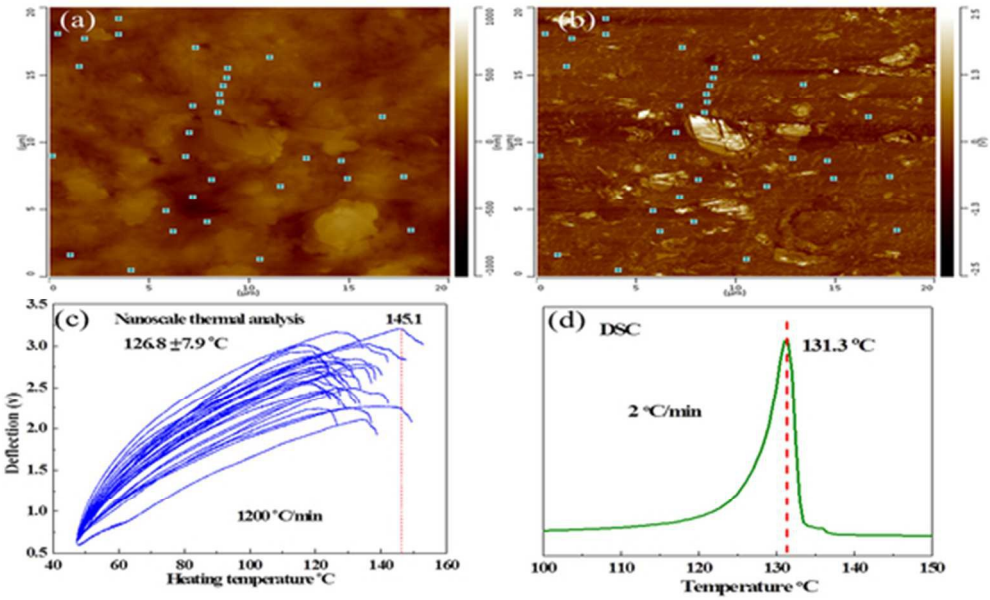

49x30mm (300 x 300 DPI)

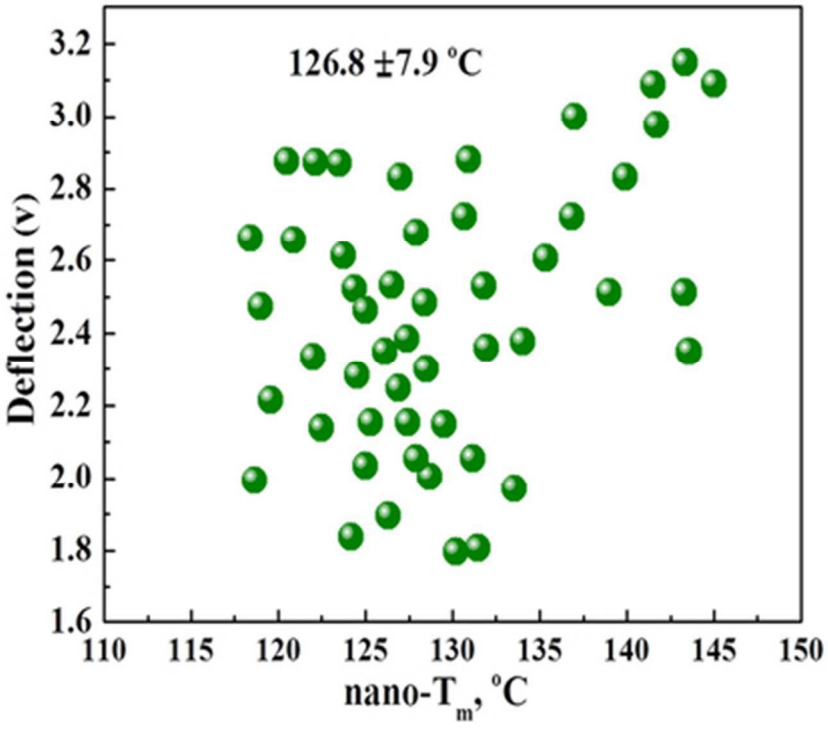

34x30mm (300 x 300 DPI)

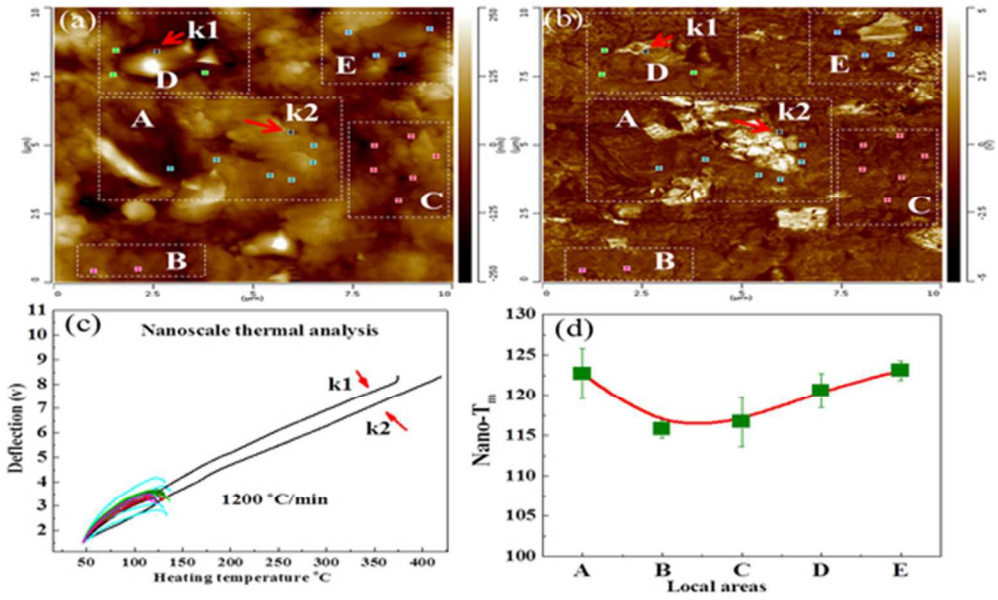

49x30mm (300 x 300 DPI)

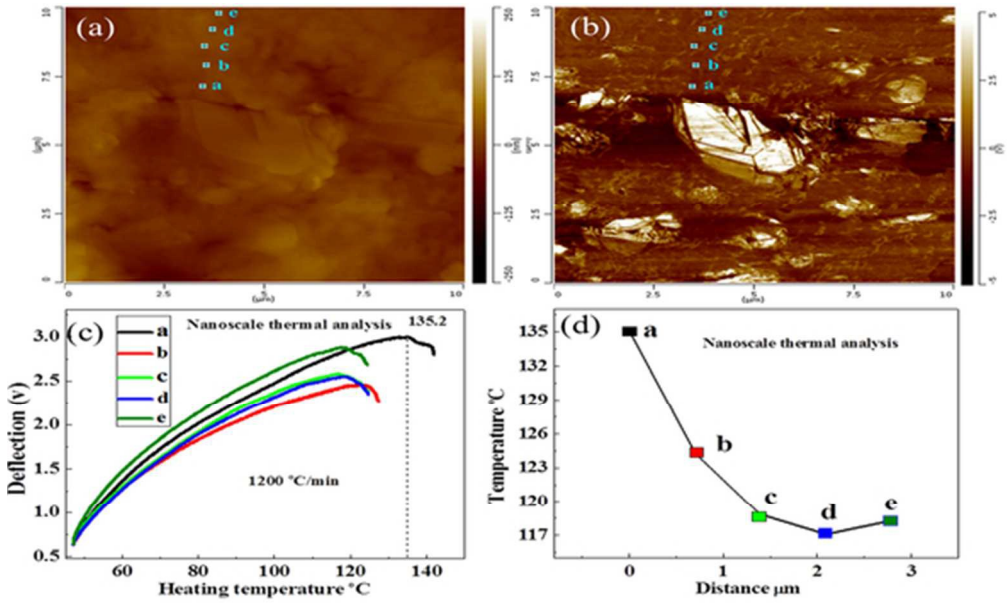

49x30mm (300 x 300 DPI)

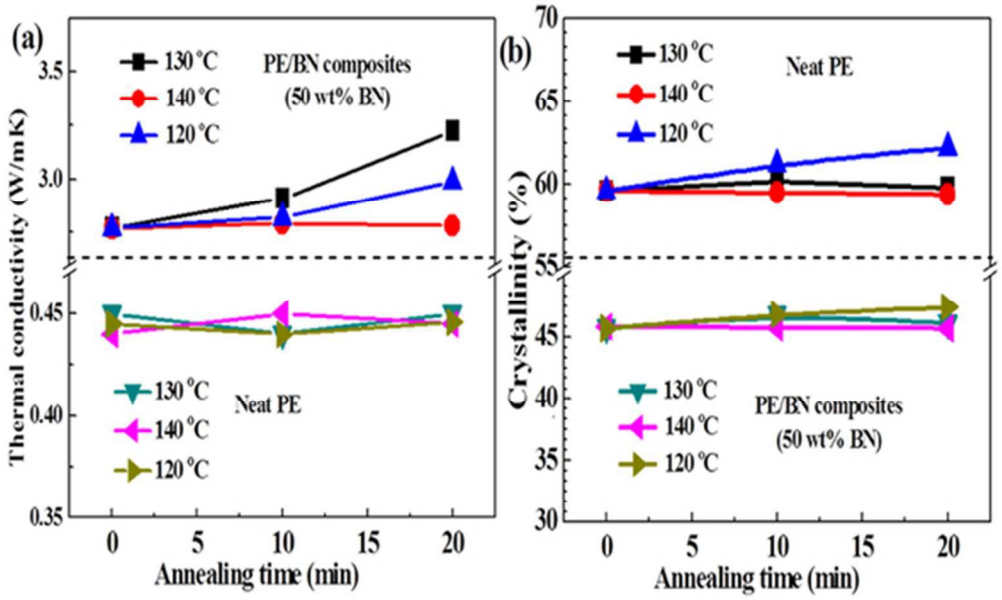

49x30mm (300 x 300 DPI)

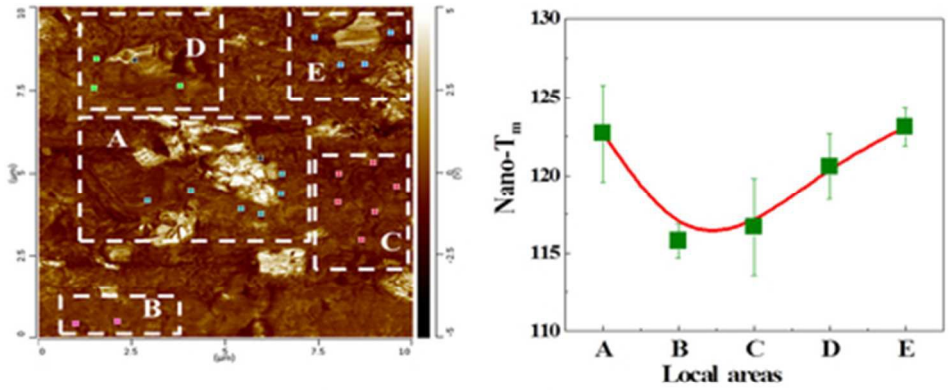

The nano-Tm of the PE near the BN aggregates was higher 4-8 °C than that in other areas.

39x19mm (300 x 300 DPI)